

The Treatment Strategies of Acid Mine Drainage Based on Resource Utilization

Mengfang Chen, Hongping Chen, Yulu Ai, Yudong Feng, Jing Li

State Key Laboratory of Soil and Sustainable Agriculture, Institute of Soil Science,
Chinese Academy of Sciences, Nanjing 210008, China

Abstract

Acid mine drainage (AMD) poses major environmental challenges due to its acidity, high sulfate, and metal concentration. This study developed multifunctional remediation materials using natural attapulgite and alkaline residues, enhancing the performance of constructed wetlands (CWs). The materials improved sulfate and metal ion removal, stabilized pollutants, and supported microbial communities, enabling long-term treatment efficiency. In-situ mineralization further converted AMD into valuable layered double hydroxides (LDHs), aiding arsenic (As) and antimony (Sb) fixation. This low-cost, sustainable approach offers promising applications for AMD remediation and industrial wastewater management, advancing green solutions for environmental protection.

Keywords: Acid mine drainage, constructed wetlands, layered double hydroxides, arsenic, antimony

Introduction

Acid mine drainage (AMD) is a persistent environmental issue caused by the oxidative leaching of sulfide minerals in mining residues such as tailings, waste rocks, and underground excavations (Kefeni *et al.* 2017). It is characterized by strong acidity, high sulfate concentrations, and elevated levels of toxic metal(loid)s (Nordstrom *et al.* 2015). Globally, AMD has severely affected water resources and ecosystems, with regions like the United States, Australia, and China facing widespread contamination due to abandoned mines (Kefeni *et al.* 2017). This widespread pollution emphasizes the urgent need for effective and sustainable AMD remediation technologies.

Traditional AMD treatment methods are classified into active and passive systems (Johnson and Hallberg 2005). Active treatments, such as chemical neutralization using lime or sodium hydroxide, are effective but often incur high operational and maintenance costs (Naidu *et al.* 2019). In contrast, passive systems like constructed wetlands (CWs) offer low-cost, energy-efficient alternatives (Skousen *et al.* 2017). However, the extreme acidity and high concentrations of metals and sulfates in AMD can harm plants and microorganisms in

CWs, reducing their treatment efficiency if not properly pre-treated. Therefore, optimizing CW configurations to improve their tolerance and purification capacity for AMD is of great scientific and practical importance.

Substrate optimization is a critical factor in improving CW performance. Organic carbon sources and inorganic media not only provide microbial attachment sites but also facilitate pollutant removal through adsorption, filtration, and complexation (Sheoran and Sheoran 2006). However, few studies have focused specifically on optimizing inorganic media in CWs. Conventional materials such as gravel and sand mainly serve to trap larger particles but are largely ineffective in removing metals and sulfate from AMD. Therefore, incorporating multifunctional materials with superior properties presents a promising strategy to improve CW efficiency in AMD treatment. In our previous studies (Chen *et al.* 2022), attapulgite-soda residue (ASR) composites showed strong metal removal and acid neutralization capacities. Combining ASR with organic carbon sources as CW substrates is expected to enhance the simultaneous removal of sulfate, metals, and acidity. However, it remains unclear



whether ASR can alleviate AMD-induced stress on plants and microorganisms within CWs. Moreover, further research is needed to clarify whether pollutant removal in ASR-based CWs is driven primarily by substrate adsorption or microbial metabolism.

Although AMD is widely recognized as a major pollution source, it is also a potential resource for valuable metal ions and sulfates (Hedrich and Johnson 2014). Harnessing AMD for resource recovery aligns with the principles of green and sustainable remediation. Studies have shown that under actual mining conditions, layered double hydroxides (LDHs)-a type of secondary mineral-can form naturally in AMD-impacted rivers (Chikanda *et al.* 2021). LDHs are considered promising adsorbents for oxygen-containing anions such as arsenate, antimonate, and chromate, owing to their high surface area, abundant hydroxyl groups, and excellent anion exchange capacity (Fang *et al.* 2021). However, most LDH synthesis methods rely on pure chemical reagents, leading to high material costs and limiting their large-scale application in water remediation (Maziarz *et al.* 2019). Given its composition, AMD can serve as a low-cost source of sulfate, Fe, Mg, and Mn for synthesizing sulfate-intercalated iron-based LDHs, potentially reducing production costs significantly. Nevertheless, the synthesis of such LDHs directly from field AMD, as well as their mechanisms for As and Sb removal, remain largely unexplored.

This study aims to develop multifunctional remediation materials by combining natural attapulgite with industrial by-product alkaline residues, evaluate their effectiveness in enhancing sulfate and metal removal, stabilizing pollutants in AMD, and supporting microbial communities in CWs. Additionally, the study explores the in-situ formation of LDHs from AMD for direct immobilization of As and Sb, providing insights into pollutant removal mechanisms and contributing to sustainable strategies for AMD remediation and resource recovery.

Methods

Materials: Attapulgite was sourced from Xuyi County, Jiangsu Province, China, and soda residue SR, a by-product of the ammonia-soda

process, was obtained from Lianyungang, Jiangsu Province. The ASR composites were prepared by mixing attapulgite and SR at a 5:5 ratio with 7.5% sodium carbonate as a binder, followed by granulation, drying at 105 °C for 12 h, and calcination at 450 °C for 2 h. AMD samples were collected from a pyrite mine in Sichuan Province, China. The AMD exhibited high sulfate (2198 mg L⁻¹) and metal concentrations (Fe 268 mg L⁻¹, Mn 66.4 mg L⁻¹, Cu 91.7 mg L⁻¹, Zn 79.8 mg L⁻¹, Cd 4.28 mg L⁻¹ and Pb 0.33 mg L⁻¹) with pH 2.08.

Construction and operation of laboratory-scaled CWs: Laboratory-scale horizontal subsurface flow constructed wetlands (HSSF-CWs) were set up in a net house in Nanjing, China, under uncontrolled environmental conditions to simulate real scenarios. Each CW consisted of a polypropylene box (57 × 26 × 42 cm) with a water inlet and outlet, filled in layers: coarse gravel, fine gravel or ASR composites mixed with organic fertilizer (2:1, v/v), soil, and overlying water. Nine *Typha* seedlings were planted in each CW after a 4-week acclimatization period. CW systems operated for 9 months in continuous flow mode with a hydraulic retention time (HRT) of 7 days. Influent and effluent water samples were collected weekly to measure pH using pH probes, and sulfate and metal concentrations using ion chromatography and inductively coupled plasma optical emission spectrometry (ICP-OES) after filtration and acidification. Soil and substrate samples were analysed post-experiment for total and chemical fractions of metals using a modified BCR sequential extraction method (Wang *et al.* 2019), X-ray diffraction (XRD), and ICP-OES. Plant photosynthetic pigments, catalase (CAT), peroxidase (POD), superoxide dismutase (SOD), and malondialdehyde (MDA) were measured spectrophotometrically. Metal concentrations in plant tissues were measured by ICP-MS. Substrate DNA was extracted for microbial community analysis via 16S rRNA sequencing. OTUs were clustered (97% similarity), and species were annotated using the RDP classifier.

Resource utilization of field AMD: Sulfate and metal ions from field-collected

AMD were used to synthesize LDHs for the direct immobilization of As and Sb within the AMD matrix. In-situ immobilization was carried out via coprecipitation in a four-necked flask. AMD samples (200 mL) containing 10.6 mg L^{-1} Sb and 7.8 mg L^{-1} As were mixed with 0.8 M NaOH under vigorous stirring at 40°C , maintaining a pH of 8.8–9.3. The resulting As- and Sb-loaded LDHs were separated, thoroughly cleaned, freeze-dried, and analyzed. Elemental composition was analyzed by ICP-MS, crystal structures by XRD, and morphology by scanning/transmission electron microscopy (SEM/TEM). Functional groups were identified using Fourier transform infrared spectroscopy (FTIR), surface area was measured via nitrogen adsorption–desorption, and surface binding energies were examined by X-ray photoelectron spectroscopy (XPS). Additionally, density functional theory (DFT) calculations were performed to explore the interactions of As and Sb with LDHs, with particular focus on anion exchange mechanisms and the potential formation of brandholzite.

Results and Discussion

Performance of CWs for AMD treatment: The effluent pH of constructed wetlands filled with gravel (CWs-G, as the control) ranged from 5.5 to 6.1 (average 5.9) during the first 200 days but gradually declined to 4.5 afterward (Fig. 1a). The sulfate concentration

showed an inverse trend, decreasing from 2096 to 1161 mg L^{-1} initially but rising to 1569 mg L^{-1} after 200 days, with an average removal efficiency of 42% (Fig. 1b). High sulfate concentrations ($> 2000 \text{ mg L}^{-1}$) have been a major challenge in AMD treatment (Fernando *et al.* 2018). Removal efficiencies for Fe, Mn, Cu, Zn, Cd, and Pb were 88%, 26%, 71%, 77%, 64%, and 60%, respectively (Fig. 1c–h). These results indicate that traditional constructed wetlands (filled with gravel and organic substrates) have limited long-term purification efficiency for AMD. In comparison, constructed wetlands filled with ASR composites (CWs-ASR) exhibited a higher effluent pH, consistently ranging from 7.7 to 8.4 throughout the operation period (Fig. 1a), meeting the pH requirement of China's Integrated Wastewater Discharge Standard ($6 < \text{pH} < 9$). Furthermore, sulfate removal efficiency substantially improved to 72%, and the removal efficiencies of all six metals exceeded 96% (Fig. 1), with concentrations meeting the Class I limits of the same standard.

Removal pathway of metals in CWs: Except for Fe and Mn, metal concentrations in wetland substrates were obviously higher than those in surface soil. In CWs-G substrates, the concentrations of Fe, Mn, Cu, Zn, Cd, and Pb were 5147, 599, 2864, 1540, 213, and 103 mg kg^{-1} , respectively (Fig. 2). The addition of composites to the substrate in CWs-ASR substantially enhanced the

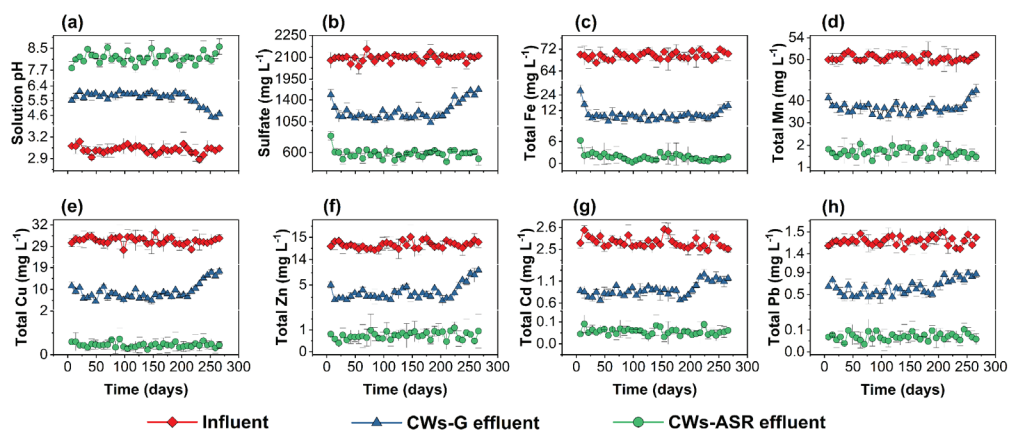


Figure 1 Temporal variations of pH (a) and concentrations of sulfate (b), total Fe (c), Mn (d), Cu (e), Zn (f), Cd (g) and Pb (h) in different CWs during the whole experiments.



removal of all metals, increasing Fe, Mn, Cu, Zn, Cd, and Pb concentrations to 6055, 2304, 4092, 2053, 329, and 172 mg kg⁻¹, respectively, representing increases of 18–285% compared to CWs-G (Fig. 2). Sequential extraction analysis revealed changes in the chemical forms of metals in soil and substrate. In CWs-G, metals primarily existed as exchangeable (14–36%), carbonate-bound (11–17%), Fe-Mn oxide-bound (31–56%), and organic/sulfide-bound forms (9–28%) (Fig. 2). However, in CWs-ASR, exchangeable metals were reduced to 1–5%, while metals associated with carbonates (19–32%) and organic/sulfides (29–34%) substantially increased (Fig. 2). Compared to CWs-G, plants in CWs-ASR exhibited substantially lower metal contents in both roots and shoots. These results indicate that the addition of composites substantially reduces the bioavailability of metals, consistent with findings from sequential extraction.

Responses of plants and microorganisms in CWs: The response of plants to AMD stress was evaluated by analyzing changes in photosynthetic pigments and biochemical

indicators in CWs-G and CWs-ASR. As shown in Fig. 3a, the concentrations of photosynthetic pigments in CWs-G plants, including chlorophyll a (1.73 mg g⁻¹), chlorophyll b (0.62 mg g⁻¹), and carotenoids (0.52 mg g⁻¹), were substantially lower than those in CWs-ASR plants (2.45, 0.93, and 0.78 mg g⁻¹, respectively). Similar trends were observed in the activities of SOD, CAT, and POD (Fig. 3b–d). Specifically, SOD (78.24 U g⁻¹), CAT (43.21 U g⁻¹), and POD (32.46 U g⁻¹) activities in CWs-G plants were markedly lower than those in CWs-ASR plants, which reached 114.56, 65.34, and 36.17 U g⁻¹, respectively. These differences indicate that plants in CWs-G experienced abiotic damage when exposed to AMD (Jia *et al.* 2020), whereas the application of composites in CWs-ASR alleviated this abiotic stress.

The microbial community diversity was higher in CWs-ASR, indicating that the application of composites promoted microbial growth, which contributed to the improved AMD treatment performance in CWs-ASR. The abundance of Proteobacteria, closely associated with sulfur cycling due to

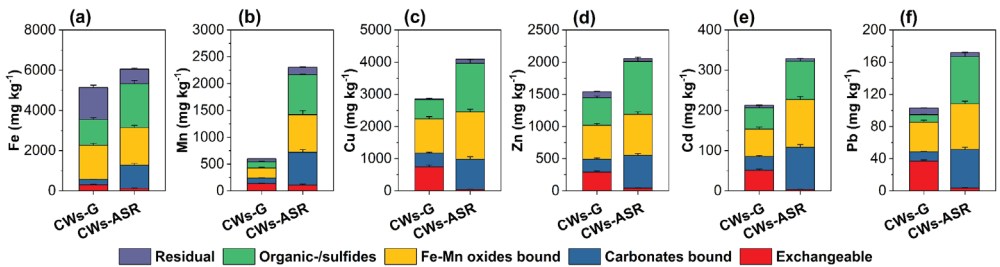


Figure 2 Metal speciation in the CWs substrates determined by sequential extraction.

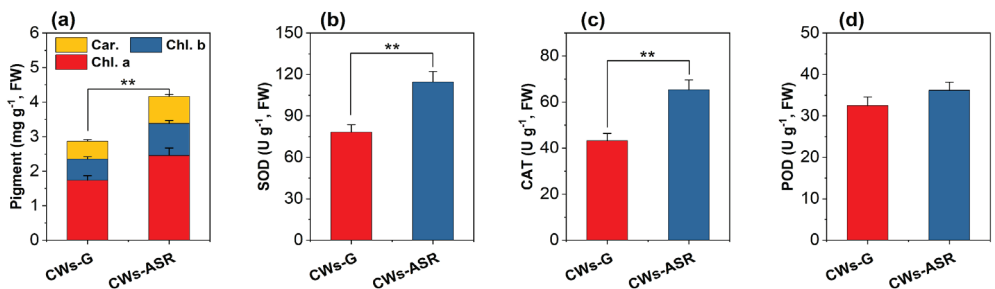


Figure 3 Variations of physiological indexes of wetland plants in different CWs, including photosynthetic pigments (a), SOD (b), CAT (c) and POD (d).

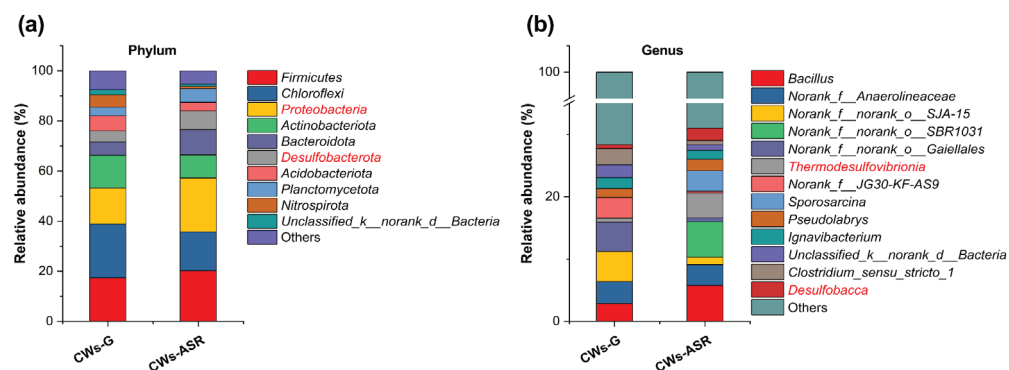


Figure 4 Percentages of community abundance in different CWs at phylum (a) and genus (b) levels.

its sulfate-reducing species (Jia *et al.* 2022), was higher in CWs-ASR (21.5%) compared to CWs-G (14.3%) (Fig. 4a). Additionally, the relative abundance of *Desulfobacterota*, critical for sulfate and metal removal (Jia *et al.* 2022), was greater in CWs-ASR (7.5%) than in CWs-G (4.4%) (Fig. 4a). At the genus level, CWs-ASR also exhibited a higher relative abundance of sulfate-reducing bacteria (SRB) (Fig. 4b). The Circos plot further highlighted the distribution of SRB genera across different wetlands. Besides *Thermodesulfovibrionia* and *Desulfobacca*, CWs-ASR had a greater relative abundance of *Desulfosarcinaceae*, *Desulfurivibrionaceae*, *Desulfatitalea*, and *Desulfosporosinus*, all of which are associated with sulfate reduction (Jia *et al.* 2022). In summary, the application of composites enhanced microbial diversity in CWs-ASR, and the increased abundance of these microorganisms likely played a key role in AMD treatment.

In situ immobilization of As and Sb containing AMD by forming LDHs: After inducing the formation of LDHs in AMD, the concentrations of Fe, Mg, sulfate, As, and Sb decreased from initial values of 1690, 1524, 2055, 7.8, and 10.6 mg L⁻¹ to 1.3, 12.4, 623, 0.006, and 0.004 mg L⁻¹, achieving reduction rates of 69.7–99.9%. Both As and Sb concentrations in the treated AMD were below the limits set by China's drinking water standards (GB 5749-2022). The desorption and TCLP tests showed dissolution rates of Fe, Mg, As, and Sb below 1%, indicating excellent chemical stability of the As/Sb-LDHs under both acidic

and alkaline conditions, with controlled risks of secondary pollution. XRD analysis of As/Sb-LDHs revealed a hydrotalcite crystalline phase (Fig. 5a). Differences in interlayer spacing were attributed to variations in the ionic radii of sulfate, As, and Sb, suggesting partial replacement of interlayer sulfate by As and Sb (Fig. 5b). New peaks in the XRD spectrum of Sb-LDH corresponded to MgSb₂(OH)₁₂·6H₂O, indicating that surface Mg ions formed complexes with Sb (Fig. 5a). FTIR spectra of As-LDHs showed weakened intensities of S-O groups at 1116 cm⁻¹ and -OH groups at 3456 cm⁻¹, alongside the appearance of an As-O band at 820 cm⁻¹, suggesting that As was captured by LDHs through complexation with -OH functional groups (Fig. 5c). In the O 1s spectra of As/Sb-LDHs, an additional As-O peak was observed, and the relative peak area of Fe/Mg-OH decreased from 49.4% to 32.3%, indicating Mg-OH bond breakage and the formation of MgSb₂(OH)₁₂·6H₂O (Fig. 5d). A reduction in Fe 2p_{3/2} and Fe 2p_{1/2} binding energies post-reaction suggested Fe-OH bond cleavage and Fe-O-As bond formation (Fig. 5d). In coexisting conditions, Sb obviously interfered with the fixation of As by LDHs, while As had no notable effect on Sb fixation. DFT calculations showed that the formation energies (E_{form}) for Sb via anion exchange and complexation were substantially lower than those for As, indicating that Sb fixation on LDHs is more favorable and explaining Sb's interference with As fixation.

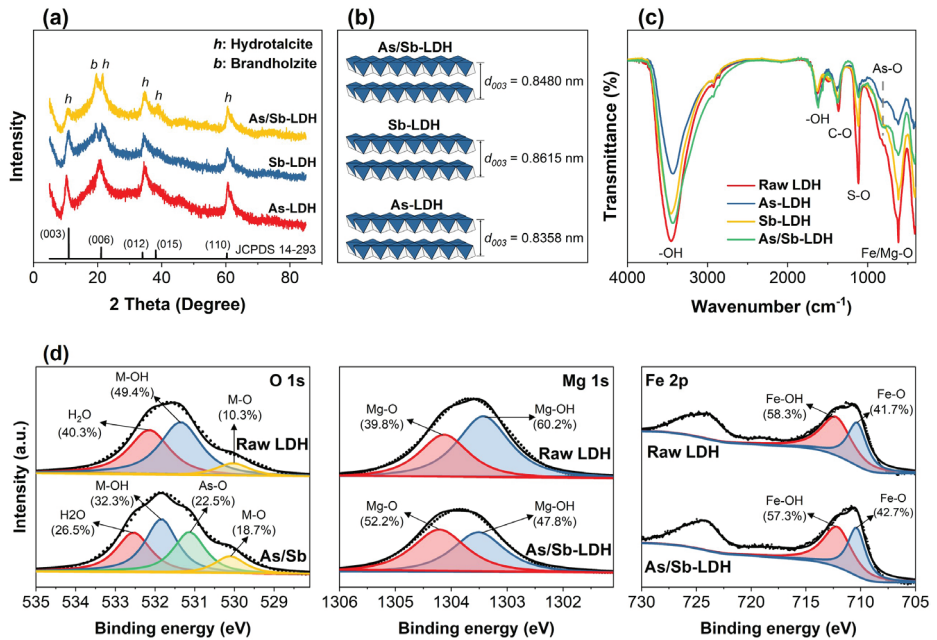


Figure 5 The X-ray diffraction patterns (a), interplanar spacing (b), FTIR spectra (c) and XPS spectra (d) of the LDHs loaded with As and/or Sb.

Conclusions

The application of ASR composites as substrates in CWs is a cost-effective and efficient method to improve AMD treatment. ASR composites neutralize AMD, reduce metal bioavailability, alleviate oxidative stress on wetland plants, and enhance microbial diversity. Sulfate-reducing bacteria (SRB) regenerates active sites on saturated ASR, further enhancing CW efficiency through synergistic adsorption and microbial sulfate reduction. The in-situ formation of LDHs in AMD is a simple and effective method for immobilizing As and Sb. The As- and Sb-loaded LDHs exhibit high chemical stability under acidic and alkaline conditions, minimizing secondary pollution risks. While Sb may interfere with As immobilization, LDH performance is largely unaffected by pH or coexisting ions. As is immobilized by anion exchange and complexation with -OH groups, whereas Sb interacts with Mg through ionic bonding. This innovative approach provides a practical solution for in-situ remediation of AMD from sulfate-rich, As- and Sb-contaminated abandoned mines.

Acknowledgements

The study was financially supported by the Natural Science Foundation of China (Grant No. 42207093) and the Natural Science Foundation of Jiangsu Province (Grant No. BK20210995). The authors thank all co-organisers for hosting the IMWA 2025 Conference.

References

- Chen HP, Ai YL, Jia YF, Li J, Gu MY, Chen M (2022) Effective and simultaneous removal of heavy metals and neutralization of acid mine drainage using an attapulgite-soda residue based adsorbent. *Sci Total Environ* 843:157120. doi:10.1016/j.scitotenv.2022.157120
- Chikanda F, Otake T, Koide A, Ito A, Sato T (2021) The formation of Fe colloids and layered double hydroxides as sequestration agents in the natural remediation of mine drainage. *Sci Total Environ* 774:145183. doi:10.1016/j.scitotenv.2021.145183
- Fang QZ, Ye SJ, Yang HL, Yang KH, Zhou JW, Gao Y, Lin QY, Tan XF, Yang ZZ (2021) Application of layered double hydroxide-biochar composites in wastewater treatment: Recent trends, modification strategies, and outlook. *J Hazard Mater* 420:126569. doi:10.1016/j.jhazmat.2021.126569



- Fernando WAM, Ilankoon IMSK, Syed TH, Yellishetty M (2018) Challenges and opportunities in the removal of sulphate ions in contaminated mine water: A review. *Miner Eng* 117:74-90. doi: 10.1016/j.mineng.2017.12.004
- Hedrich S, Johnson DB (2014) Remediation and selective recovery of metals from acidic mine waters using novel modular bioreactors. *Environ Sci Technol* 48:12206-12212. doi:10.1021/es5030367
- Jia LX, Liu H, Kong Q, Li M, Wu SB, Wu HM (2020) Interactions of high-rate nitrate reduction and heavy metal mitigation in iron-carbon-based constructed wetlands for purifying contaminated groundwater. *Water Res* 169:115285. doi:10.1016/j.watres.2019.115285
- Jia YY, Wang PD, Ou YY, Yan YJ, Zhou SN, Sun LP, Lu H (2022) Insights into the microbial response mechanisms to ciprofloxacin during sulfur-mediated biological wastewater treatment using a metagenomics approach. *Water Res* 223:118995. doi:10.1016/j.watres.2022.118995
- Johnson DB, Hallberg KB (2005) Acid mine drainage remediation options: A review. *Sci Total Environ* 338:3-14. doi:10.1016/j.scitotenv.2004.09.002
- Kefeni KK, Msagati TAM, Mamba BB (2017) Acid mine drainage: Prevention, treatment options, and resource recovery: A review. *J Clean Prod* 151:475-493. doi:10.1016/j.jclepro.2017.03.082
- Maziarz P, Matusik J, Straczek T, Kapusta C, Woch WM, Tokarz W, Radziszewska A, Leiviska T (2019) Highly effective magnet-responsive LDH-Fe oxide composite adsorbents for As(V) removal. *Chem Eng J* 362:207-216. doi:10.1016/j.cej.2019.01.017
- Naidu G, Ryu S, Thiruvengkatachari R, Choi Y, Jeong S, Vigneswaran S (2019) A critical review on remediation, reuse, and resource recovery from acid mine drainage. *Environ Pollut* 247:1110-1124. doi:10.1016/j.envpol.2019.01.085
- Nordstrom DK, Blowes DW, Ptacek CJ (2015) Hydrogeochemistry and microbiology of mine drainage: An update. *Appl Geochem* 57:3-16. doi: 10.1016/j.apgeochem.2015.02.008
- Sheoran AS, Sheoran V (2006) Heavy metal removal mechanism of acid mine drainage in wetlands: A critical review. *Miner Eng* 19:105-116. doi:10.1016/j.mineng.2005.08.006
- Skousen JG, Zipper CE, Rose A, Ziemkiewicz PF, Nairn R, McDonald LM, Kleinmann RL (2017) Review of passive systems for acid mine drainage treatment. *Mine Water Environ* 36:133-153. doi:10.1007/s10230-016-0417-1
- Wang J, Wang PM, Gu Y, Kopittke PM, Zhao FJ, Wang P (2019) Iron-manganese (oxyhydro)oxides, rather than oxidation of sulfides, determine mobilization of Cd during soil drainage in paddy soil systems. *Environ Sci Technol* 53:2500-2508. doi: 10.1021/acs.est.8b06863